Citation: A. González, M. Aranda, G. López-Nicolás, C. Sagüés. Robust stability analysis of formation control in local frames under time-varying delays and actuator faults. Journal of the Franklin Institute, vol. 356, no. 2, pp. 1131-1153, 2019.

Robust stability analysis of formation control in local frames under time-varying delays and actuator faults

Antonio González[a], Miguel Aranda[b], Gonzalo López-Nicolás[a], Carlos Sagüés[a]

[a] *Inst. de Investigación en Ingeniería de Aragón - Universidad de Zaragoza, C /María de Luna 1, E-50018 Zaragoza, Spain (e-mail: angonsor@gmail.com,gonlopez@unizar.es,csagues@unizar.es).*
[b] *SIGMA Clermont, Institut Pascal, 4 Avenue Blaise Pascal, 63178 Aubière Cedex, France (e-mail: miguel.aranda@sigma-clermont.fr)*

Abstract

This paper investigates the robust stability of a multiagent system moving to a desired rigid formation in presence of unknown time-varying communication delays and actuator faults. Each agent uses relative position measurements to implement the proposed control method, which does not require common coordinate references. However, the presence of time delays in the measurements, which is inherent to the communication links between agents, has a negative impact in the control system performance leading, in some cases, to instability. Furthermore, the robust stability analysis becomes more complex if failures on actuators are taken into account. In addition, delays may be subject to time variations, depending on network load, availability of communication resources, dynamic routing protocols, or other environmental conditions. To cope with these problems, a sufficient condition based on Linear Matrix Inequalities (LMI) is provided to ensure the robust asymptotic convergence of the agents to the desired formation. This condition is valid for any arbitrarily fast time-varying delays and actuator faults, given a worst-case point-to-point delay. Finally, simulation results show the performance of the proposed approach.

Keywords: Multiagent systems, Formation stabilization, Robust control theory, Time-varying delay, Linear Matrix Inequality (LMI)

1. Introduction

1.1. Background and motivation

The problem of controlling a multiagent system can be useful in a broad array of applications. To mention a few: autonomous multivehicle control [1], entertainment [2], search and rescue missions [3], etc. A key issue in this domain that receives particular interest is how to stabilize and maintain a geometrical formation shape in a distributed manner [4, 5]. Such shapes can be needed so as to ensure the team members can interact (via sensing or communications) suitably or satisfy geometric task constraints given by the environment, or for safety considerations (e.g., avoidance of collisions).

Two main approaches have been proposed depending on how the formation is defined: (i) in terms of absolute positions the agents must reach [6, 7], and (ii) in terms of relative interagent distances [8] or relative interagent position vectors [9, 10, 11]. In particular, it is of practical interest to consider that only relative position measurements between agents are available, and that the agents' measurements frames are not equally oriented [12, 13, 14]. The main advantage in this latter case is that no global reference has to be shared by the agents, which increases the flexibility and autonomy. For instance, they can operate in a GPS-denied environment by using the locally referred information coming from their independent onboard sensors. However, this scenario involves significant challenges: linear consensus-based controllers cannot be used in general, and control analysis and stability guarantees become harder to provide.

The coordinate-free formation control strategy proposed in [14] has the advantage of achieving global convergence to a unique rigid shape in absence of a global coordinate system and leader agents, which brings more robustness and flexibility. The misalignment between orientation references is addressed by introducing in the cost function a rotation angle, on which the agents implicitly agree, capturing the method's independence of any global reference. With this motivation, we focus on the control framework of [14] to carry out our study.

A relevant issue to take into account in the stability analysis of formation control systems is the presence of time delays [15, 16], which appear due to multi-hop communication between agents. Indeed, our multiagent team constitutes a networked system, in which the agents interact via communications. This connects with the important field of networked control systems. Various communications-related aspects have fundamental effects in control

performance, as reviewed in [17]. Some current challenges in the study of multi-agent networked systems include addressing time-varying time delays (as done here), switching network topologies, impulsive behaviors, or temporal constraints for control execution. Aside from formation control, other problems of interest include tracking and consensus [18, 19, 20], stability and robust performance analysis under actuator degradation or failures [21, 22] and disturbance rejection in the context of stochastic systems [23].

It is worthwhile mentioning that communication delays in networked systems are subject to time variations depending on different factors such as time-varying network load, bandwith/communication resources availability, scheduling policies in the dynamic routing protocols, or possible random network failures [24], etc. Time-varying delays on control systems have been mainly investigated under two approaches: (i) Lyapunov-Krasovskii functionals [25, 26] and (ii) Input/Output approach/Small Gain Theorem [27, 28]. Indeed, for systems with time-varying uncertainties, input/output approaches allow finding an equivalent description by means of interconnected system modeling, where the feedback system contains all sources of uncertainties of the original system. In this way, the stability analysis can be addressed via small-gain theory, exploiting the interconnected nature of the transformed system. Other interesting applications where interconnected nonlinear systems and small-gain approaches are involved can be found in the analysis of stochastic network systems [29].

In the context of multiagent systems, some contributions can be found in the literature which face up with the robust stability analysis in presence of time-varying delays [30, 31, 32]. However, such approaches consider that all the agents share a common orientation reference, rely on central coordinators/leader agents, or assume continuously differentiable functions for time-varying delays with restrictions on their maximum time-derivative. Notably, the work presented here eliminates these assumptions, which results in increased flexibility and applicability of the proposed method.

On the other hand, in [14], the analysis of time delays in the stability of a coordinate-free formation control system is addressed by providing an upper bound for time delays so that the overall system asymptotically converges to the desired geometric configuration. Nevertheless, the following limitations on its applicability can be found: (i) delays must be time-constant, (ii) prior knowledge of the boundedness of the total disturbance created by the time-delays is required [14, Assumption A2] and (iii) actuator faults are not considered.

Therefore, we believe that the robust stability analysis of the coordinate-free/leaderless multiagent system to the case of unknown arbitrarily fast time-varying communication delays and possible failures on actuators is interesting from a practical point of view. It is worthwhile to recall that the interconnected [33] and the nonlinear nature of the underlying control system, combined with the presence of time-varying delays and actuator faults, makes the robust stability analysis a complex issue, which motivates our study.

1.2. Contribution

We extend the stability analysis of the coordinate-free formation control strategy of multiagent systems in [14] to the case of unknown time-varying communication delays and actuator faults. To this end, we provide a sufficient condition based on Linear Matrix Inequalities (LMI) [34] which ensures the asymptotic convergence of the coordinate-free formation control system to the desired geometric configuration. Furthermore, we give an algorithm to find the maximum upper bound delay (hereinafter, referred to as worst-case point-to-point delay) to guarantee the stability of the multiagent formation control system. The following aspects are noteworthy:

- The estimation of the worst-case point-to-point delay does not require prior knowledge of the relative boundedness of the total disturbance due to time-delays with respect to the tracking formation error (as opposed to [14, Assumption A2]). The interest of eliminating such assumption lies on the difficulty of having a reliable estimation of such bound in advance.

- Time delays are allowed to be arbitrarily fast time-varying. In other words, there are no constraints on their time-derivative, which might be also difficult to estimate a priori. Further advantages of this key aspect are discussed later (Remark 3).

- The robustness against time-varying delays and actuator faults is analyzed in a single framework, which is generally difficult to prove in multiagent systems under coordinate-free formation control strategies.

1.3. Organization

The remainder of the paper is organized as follows: Section 2 describes the problem statement and gives the preliminary results and notation. Section 3

finds a delay-free model description of the multiagent system, which is used in Section 4 to obtain the proposed methodology for robust stability analysis. Simulation results are provided in Section 5 and, finally, conclusions and perspectives are gathered in Section 6.

2. Problem statement and preliminaries

Consider the following multiagent system formed by N agents, where the kinematics of each agent is modeled as a single integrator:

$$\dot{q}_i = f_i u_i, \qquad i = 1, ..., N, \tag{1}$$

where f_i is introduced to consider possible actuators faults, which are modeled as in [21]:

$$f_i = f_i(t) = \begin{cases} 1: & no\ actuator\ fault, \\ 0 < \underline{f}_i \leq \tilde{f}_i(t) \leq \overline{f}_i \leq 1: & actuator fault, \end{cases} \tag{2}$$

where $\tilde{f}_i(t)$ is an unknown parameter which denotes the loss of effectiveness of the f_{th} actuator, and $\underline{f}_i, \overline{f}_i$ are time-constant and known values. The parameter $q_i = [q_{x,i}, q_{y,i}]^T$ is the 2-D vector position of the agent $i = 1, \cdots, N$, expressed in an arbitrary reference frame, and u_i is the control action. For each pair of agents $k, i \in [1, ..., N] \times [1, ..., N], k \neq i$, we define $q_{ki} = q_k - q_i$ and c_{ki} respectively as the current and the desired relative position between them. The target formation is defined by the overall set of vectors c_{ki}. The difference between the current and desired relative position between agents k and i is captured by means of the error vector d_{ki} defined as:

$$\begin{aligned} d_{ki} &= q_{ki} - R(\alpha) c_{ki}, \\ R(\alpha) &= \begin{bmatrix} cos(\alpha) & -sin(\alpha) \\ sin(\alpha) & cos(\alpha) \end{bmatrix}, \end{aligned} \tag{3}$$

where α is the rotation angle of the desired reference pattern which minimizes the following cost function:

$$J = \sum_k \sum_j ||q_{kj} - R(\alpha) c_{kj}||^2 . \tag{4}$$

Specifically, the rotation angle has the following value [1]:

$$\alpha = atan2\left(\sum_k \sum_j q_{kj}^T c_{kj}^{\perp},\ \sum_k \sum_j q_{kj}^T c_{kj}\right), \tag{5}$$

where $c_{kj}^{\perp} = \begin{bmatrix} -c_{y,kj} & c_{x,kj} \end{bmatrix}^T$.

Let us formulate the following assumptions that will be used in our analysis:

Assumption 1 *The following condition holds:* $\left|\sum_k \sum_j q_{kj}^T c_{kj}\right| \geq H,\ \forall t \geq 0$, *where*

$$H = \frac{1}{2}\left(min\left(\left|\sum_k \sum_j q_{kj}^T(t=0) c_{kj}\right|,\ \sum_k \sum_j ||c_{kj}||^2\right)\right). \tag{6}$$

The motivation of this assumption is discussed later, in Remark 5.

Assumption 2 *The communication topology is complete, that is, all the agents* $1 \leq i \leq N$ *receive the measurements of the relative positions vectors of their neighborhood:* $q_{ki},\ \forall k \in 1, ..., N,\ k \neq i$.

Assumption 3 *All the measurements of the relative positions* q_{ki} *received by agent* i *may be affected by unknown time-varying delays* $\tau_{ki}(t)$. *The delays are not necessarily symmetric* ($\tau_{ki}(t) \neq \tau_{ik}(t)$), *and not necessarily continuously differentiable functions.*

Definition 1 *Let us define the upper bounds for delays* $\bar{\tau}_{ki} :\ \tau_{ki}(t) \leq \bar{\tau}_{ki}$, *and the worst-case point-to-point delay* δ *as* $\delta = max_{k,i}\left(\bar{\tau}_{ki}\right)$. *The normalized upper bound delays are defined as* $\hat{\tau}_{ki} = \bar{\tau}_{ki}/\delta$. *Note that* $0 \leq \hat{\tau}_{ki} \leq 1$ *and* $\tau_{ki}(t) \leq \bar{\tau}_{ki} = \delta\hat{\tau}_{ki} \leq \delta$.

Remark 1 *Assumption 2 does not imply that all the communication links are necessarily active at the same time during control execution. In other*

[1] The *atan2(a,b)* function gives the solution of $\alpha = arctan(a/b)$, given two scalars a, b, for which the angle α is in the quadrant that corresponds to the signs of the two inputs arguments a, b.

words, if the communication link between agents k and i fails, the relative interagent position between both agents can be transmitted to agent k and agent i via multi-hop communication protocols through one or multiple different communication links involving other neighbor agents. Therefore, it is reasonable to consider different upper bounds $\bar{\tau}_{ki}:\ \tau_{ki}(t) \leq \bar{\tau}_{ki}$, depending on the number of intermediate agents involved in the measurements exchange between both agents. In this way, the conservatism in the estimation of the worst-case point-to-point delay δ can be reduced by taking advantage of prior knowledge of the communication graph and the multi-hop protocol. Note also that each $\bar{\tau}_{ki}$ is related to δ through the normalized values $\hat{\tau}_{ki}$, given in Definition 1.

Following the ideas on [14], the rotation angle is estimated by each agent by adapting the expression (5) to the available delayed measurement data:

$$\alpha_i^{\tau} = atan2\left(\sum_k \sum_j \left(q_{ki}^{\tau_{ki}} - q_{ji}^{\tau_{ji}}\right)^T c_{kj}^{\perp},\ \sum_k \sum_j \left(q_{ki}^{\tau_{ki}} - q_{ji}^{\tau_{ji}}\right)^T c_{kj}\right), \qquad (7)$$

where $q_{ki}^{\tau_{ki}} \equiv q_{ki}\left(t - \tau_{ki}(t)\right)$, $q_{ji}^{\tau_{ji}} \equiv q_{ji}\left(t - \tau_{ji}(t)\right)$. In the sequel, the superscript τ in α_i^{τ} (and other possible terms) denotes dependence on time-delayed data.

The coordinate-free control strategy which is proposed in our analysis is the following static error feedback control:

$$u_i = K_c \sum_k d_{ki}^{\tau} = K_c \sum_k \underbrace{\left(q_{ki}^{\tau_{ki}} - R(\alpha_i^{\tau}) c_{ki}\right)}_{d_{ki}^{\tau}}. \qquad (8)$$

where $K_c > 0$ is the control gain, and d_{ki}^{τ} is the error defined in (3) affected by time delays. A key property of the control law (8) is that it can be computed by each agent in its own independently oriented local reference frame [14].

From (1), it can be deduced that $\dot{q}_{ji} = \dot{q}_j - \dot{q}_i = f_j u_j - f_i u_i$. Replacing u_j and u_i from control law (8), the following dynamics equations are obtained for the multiagent formation control system:

$$\dot{q}_{ji} = K_c \left(f_j \sum_k d_{kj}^{\tau} - f_i \sum_k d_{ki}^{\tau}\right), \quad [j,i] = [1,...,N] \times [1,...,N], j \neq i \quad (9)$$

Objective statement: find a systematic methodology to obtain the maximum worst-case point-to-point delay δ (see Definition 1), under which the multiagent formation control system (9) is stable, for any unknown and arbitrarily

fast time-varying delay pattern satisfying $\tau_{ki}(t) \leq \bar{\tau}_{ki} \leq \delta,\ \forall k, i$ and actuators faults modeled as (2).

2.1. Preliminary notation

The following notations are used: R^n and $R^{m\times n}$ denote, respectively, the n dimensional Euclidean space and the set of all $m \times n$ real matrices. The superscript "T" denotes matrix transposition. The notation $X > 0$ (respectively, $X < 0$), where X is a symmetric matrix, means that X is positive definite (respectively, positive negative). The symbols I_n, 0_n and $0_{m\times n}$ stand for the $n \times n$ identity matrix, the null $n \times n$ matrix and the null $m \times n$ matrix, respectively. Given a vector v, we denote $diag(v)$ as a diagonal matrix whose diagonal entry is v. Given matrices $A_1, \cdots, A_n$, we define $diag(A_1, ..., A_n)$ as the corresponding block diagonal matrix. The symbol $\otimes$ stands for the Kronecker product. We denote the set of positive integers as $\mathcal{N} = \{1, 2, \cdots\}$. Given $m \times n$ scalars $t_{11}, t_{12}, ..., t_{mn}$, we define $[t_{ij}]_{m\times n}$ as the corresponding $m \times n$ matrix. Conversely, given a matrix $T = [t_{ij}]_{m\times n}$, we denote $col(T)$ as a $m \cdot n$ column vector formed by its entries ordered as $[t_{11}, t_{12}, ..., t_{mn}]$. For any integer $n > 1$ and $1 \leq p \leq n$, the symbol $\mathcal{I}_n^p$ defines a $n - 1 \times n$ matrix which is constructed from the identity matrix I_n by removing its p_{th} row (for instance $\mathcal{I}_3^2 = \begin{bmatrix} 1 & 0 & 0 \\ 0 & 0 & 1 \end{bmatrix}$).

Note that we can rewrite $f_i(t)$ in (2) as the following convex combination:

$$f_i(t) = \begin{cases} 1: & no\ actuator\ fault, \\ f_i(t) = \tilde{\lambda}_i(t)\underline{f}_i + (1 - \tilde{\lambda}_i(t))\overline{f}_i: & actuator fault. \end{cases}, \qquad (10)$$

where $\tilde{\lambda}_i(t) = \frac{\overline{f}_i - f_i(t)}{\overline{f}_i - \underline{f}_i}$. Let n_f be the number of faulty actuators and the positive set of integers $0 < p_1 < p_2 < ... < p_{n_f} \leq N$ be the indices of each faulty actuator. Then, we define the vectors $\underline{f^*} = \begin{bmatrix} \underline{f}_{p_1} & \cdots & \underline{f}_{p_{n_f}} \end{bmatrix}^T$, $\overline{f^*} = \begin{bmatrix} \overline{f}_{p_1} & \cdots & \overline{f}_{p_{n_f}} \end{bmatrix}^T$ and the matrices $\mathcal{L} \in \{0, 1\}^{N\times n_f}$, $\mathcal{V} \in \{0, 1\}^{N\times N-n_f}$, built both from the identity matrix I_N by removing the rows whose position correspond to the non-faulty actuator indices (for $\mathcal{L}$) and the faulty actuator

ones (for $\mathcal{V}$). Also, define the matrix $\bar{\pi} \in \{0,1\}^{2^{n_f} \times n_f}$:

$$\bar{\pi} = \begin{bmatrix} \bar{\pi}_1 \\ \bar{\pi}_2 \\ \bar{\pi}_3 \\ \cdots \\ \bar{\pi}_{2^{n_f}} \end{bmatrix} = \begin{bmatrix} \pi_{1,1} & \pi_{1,2} & \cdots & \pi_{1,n_f} \\ \pi_{2,1} & \pi_{2,2} & \cdots & \pi_{2,n_f} \\ \pi_{3,1} & \pi_{3,2} & \cdots & \pi_{3,n_f} \\ \cdots & \cdots & \cdots & \cdots \\ \pi_{2^{n_f},1} & \pi_{2^{n_f},2} & \cdots & \pi_{2^{n_f},n_f} \end{bmatrix} = \begin{bmatrix} 0 & 0 & \cdots & 0 \\ 1 & 0 & \cdots & 0 \\ 0 & 1 & \cdots & 0 \\ \cdots & \cdots & \cdots & \cdots \\ 1 & 1 & \cdots & 1 \end{bmatrix}. \quad (11)$$

Thus, $f_i(t)$ in (2) can be written as a polytope: $f_i(t) = \sum_{f=1}^{2^{n_f}} \lambda_f(t) \hat{f}_f$, formed by the convex combination of the vertices $\hat{f}_f,\ f = 1, ..., 2^{n_f}$ given below:

$$\hat{f}_f = \mathcal{L}\left(\underline{f^*} + diag\left(\bar{\pi}^f\right)\left(\overline{f^*} - \underline{f^*}\right)\right) + \mathcal{V} \cdot 1_{\left(N-n_f\right)\times 1}, \quad (12)$$

$$\lambda_f(t) = \Pi_{s=1}^{n_f}\left(\left(1-\pi_{f,s}\right)\tilde{\lambda}_{p_s}(t) + \pi_{f,s}\left(1-\tilde{\lambda}_{p_s}(t)\right)\right).$$

2.2. Preliminary results

Definition 2 *[35] Given the system M with input/output $e(t)$ and $y(t)$ respectively, the H_∞ norm of system M represents the largest possible $\mathcal{L}_2$-gain provided by the system under zero initial conditions:*

$$||M||_\infty = sup_{||e||_2 \neq 0} \frac{||y||_2}{||e||_2},\ \forall e \in \mathcal{L}_2 \quad (13)$$

where $\mathcal{L}_2 = \{e(t) : \int_0^\infty ||e(s)||^2 ds < \infty\}$ denotes the set of square integrable signals, and $||e||_2$ stands for the $\mathcal{L}_2$ norm of the input signal $e(t)$, defined as $||e||_2 = \sqrt{\int_0^\infty ||e(s)||^2 ds}$.

Lemma 1 *[36] Consider the operator $\Delta_F := (\Delta_d - 1) \circ \frac{1}{s}$, where Δ_d is the time-varying operator: $\Delta_d(v) = v(t - \tau(t))$, $\tau(t)$ is a time-varying delay, which satisfies $0 \leq \tau(t) \leq \bar{\tau}$, the symbol $\circ$ denotes the Schur product, and $\frac{1}{s}$ denotes the integration operator. Then, the $\mathcal{L}_2$-induced norm of Δ_F is bounded by $\bar{\tau}$.*

2.2.1. Scaled Small Gain Theorem

The most elemental notion on the Scaled Small Gain (SSG) theorem is given in this section (further details can be found in [15], Chapter 8). Consider an interconnected system consisting of two subsystems:

$$(\mathcal{S}_1):\ y(t) = Me(t), \quad (\mathcal{S}_2):\ e(t) = \Delta y(t) \quad (14)$$

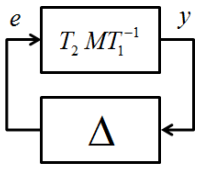

Figure 1: Interconnected system: M is a known system, and Δ is some unknown unitary norm-bounded system, which contains all sources of time-delays variations. Matrices T_1, T_2 are free and must satisfy $T_1\Delta = \Delta T_2$.

where $e \in \mathcal{R}^{n_e}$, $y \in \mathcal{R}^{n_y}$. The forward system $\mathcal{S}_1$ is a known system with operator M mapping e and y. The feedback system $\mathcal{S}_2$ is an unknown system with operator $\Delta : y \to e$ having unitary norm $||\Delta||_\infty \leq 1$. A sufficient condition for the robust asymptotic stability of the interconnection in (14) is given as follows:

Theorem 1 *(Scaled Small Gain Theorem)[15] The interconnected system on Fig. 1 is robustly stable for any interconnected time-varying uncertain system* Δ *with* $||\Delta||_\infty \leq 1$ *if the following two conditions hold: (i) The system* M *is internally stable and (ii) there exist nonsingular matrices* T_1, T_2 *such that* $T_1\Delta = \Delta T_2$ *and* $||T_2 M T_1^{-1}||_\infty < 1$.

Indeed, provided that such free matrices T_1, T_2 exist, satisfying $T_1\Delta = \Delta T_2$, it can be seen that: $\Delta = T_1^{-1}\Delta T_2$. It is straighforward that: (i) $T_1 = T_2$ if Δ is square and (ii) T_1, T_2 are of block diagonal structure if Δ is also block diagonal.

3. Delay-free model description

Notice that the nonlinear nature of the control strategy (8), along with time-varying delays on the measurements, makes the stability analysis a complex issue. To overcome this challenge, we obtain a delay-free model for the multiagent formation control system (1) and (8), consisting of the interconnection of two systems (see Fig. (1)). The underlying idea is to embed all sources of time-varying uncertainties coming from delays into the uncertain feedback system Δ through the introduction of some *artificial* inputs/outputs ($e(t)$ and $y(t)$ respectively), suitably defined such that $||\Delta||_\infty \leq 1$. In this way, we will be ready to cope with the robust stability analysis of the multiagent formation control system (9) by applying small gain theory.

Lemma 2 *The multiagent formation control* (1) *and* (8) *described by the closed-loop state-space realization* (9) *converges to the desired formation if the following interconnected system is robustly stable:*

$$\left[\frac{\dot{\hat{q}}}{y}\right] = \underbrace{\left[\begin{array}{c|c} K_c\mathcal{A}_s & K_c\mathcal{B}_s L_\delta \\ \hline L_K\mathcal{C}_s & L_K\mathcal{D}_s L_\delta \end{array}\right]}_{M} \left[\frac{\hat{d}}{e}\right], \qquad e = \Delta y \tag{15}$$

where Δ *is the uncertain feedback system, which satisfies* $||\Delta||_\infty \leq 1$*, and*

$$\begin{aligned}
&q_s^T = \begin{bmatrix} q_{21}^T & \cdots & q_{N1}^T \end{bmatrix}, \quad d_s^T = \begin{bmatrix} d_{21}^T & \cdots & d_{N1}^T \end{bmatrix}, \qquad (16)\\
&L_\delta = \begin{bmatrix} \delta I_{2\bar{N}} & 0 \\ 0 & I_{2N} \end{bmatrix}, \; L_K = \begin{bmatrix} K_c I_{2\bar{N}} & 0 \\ 0 & I_N \end{bmatrix},\\
&(\mathcal{A}_s, \mathcal{B}_s, \mathcal{C}_s, \mathcal{D}_s) = \sum_{f=1}^{2^{n_f}} \lambda_f(t) \left(\hat{\mathcal{A}}_{s,f}, \hat{\mathcal{B}}_{s,f}, \hat{\mathcal{C}}_{s,f}, \hat{\mathcal{D}}_{s,f}\right),\\
&\hat{\mathcal{A}}_{s,f} = \mathcal{T}^+ \hat{\bar{A}}_f \mathcal{T}, \quad \hat{\mathcal{B}}_{s,f} = \mathcal{T}^+ \left[\hat{\bar{B}}_{q,f} \qquad \hat{\bar{B}}_{R,f}\right], \qquad (17)\\
&\hat{\mathcal{C}}_{s,f} = \begin{bmatrix} \hat{\bar{A}}_f \mathcal{T} \\ 0_{N\times 2(N-1)} \end{bmatrix} \quad \hat{\mathcal{D}}_{s,f} = \begin{bmatrix} \hat{\bar{B}}_{q,f} & \hat{\bar{B}}_{R,f} \\ \bar{D} & 0_{N\times 2N} \end{bmatrix},
\end{aligned}$$

$$\begin{aligned}
&\mathcal{T}^+ = \begin{bmatrix} I_{N-1} & 0_{N-1\times \bar{N}-N+1} \end{bmatrix} \otimes I_2, \qquad \bar{N} = N(N-1), \qquad (18)\\
&\mathcal{T} = (Q_1 - Q_2) \begin{bmatrix} 0_{N-1\times 1} & I_{N-1} \end{bmatrix}^T \otimes I_2, \qquad \hat{\bar{A}}_f = \left(\hat{Q}_f \otimes 1_{1\times N-1}\right) \otimes I_2, \qquad ,\\
&\hat{\bar{B}}_{q,f} = \left(\left(\hat{Q}_f \otimes 1_{1\times N-1}\right) \cdot Q_3 \cdot \bar{T}\right) \otimes I_2, \qquad \hat{\bar{B}}_{R,f} = -\left(\hat{Q}_f \cdot diag\left(\bar{h}\right)\right) \otimes I_2,\\
&\bar{D} = \left(I_N \otimes 1_{1\times 2N-2)}\right) \cdot diag\left((Q_1 \otimes I_2) \cdot \bar{c}\right) \cdot \left(\bar{T} \otimes I_2\right),
\end{aligned}$$

$$\begin{aligned}
&\hat{Q}_f = (Q_1 - Q_2) \cdot diag\left(\hat{f}_f\right), \qquad (19)\\
&Q_1^T = \left[\left(\mathcal{I}_N^1\right)^T, \cdots, \left(\mathcal{I}_N^N\right)^T\right], \quad Q_2 = I_N \otimes 1_{N-1\times 1}, \quad Q_3 = diag\left(\mathcal{I}_N^1, \cdots, \mathcal{I}_N^N\right),\\
&\bar{T} = diag\left(col\left(\left[\hat{\tau}_{ij}\right]_{N,N}^T\right)\right), \quad \bar{c} = \left[\textstyle\sum_j c_{1j}^{\perp T}, \cdots, \sum_j c_{Nj}^{\perp T}\right]^T,\\
&\bar{h} = \begin{bmatrix} h_1 & \cdots & h_N \end{bmatrix}^T, \; h_{1\leq i\leq N} = \frac{1}{H}\left|\left|\sum_k c_{ki}\right|\right|,
\end{aligned}$$

where $\hat{f}_f$ *and* $\lambda_f(t)$ *are defined in* (12), $\mathcal{I}_N^p$, $p = 1, \cdots, N$ *are defined in subsection 2.1, and* H *is defined in* (6).

Proof: With the aim to put all sources of time-varying uncertainties due to time delays into a feedback unitary norm-bounded system (namely Δ), we define the inputs $e(t)$ and outputs $y(t)$ such that $e(t) = \Delta y(t)$. In (8), it is possible to clearly distinguish the following two terms affected by time-delays: $q_{ki}^{\tau_{ki}}$ and $R(\alpha_i^\tau)\sum_k c_{ki}$, respectively. Let us proceed with each of them:

(i) Input/output definition for $q_{ki}^{\tau_{ki}}$*:* For each delayed position measurement $q_{ki}^{\tau_{ki}}$, we define the input $e_{q,ki}$ and output $y_{q,ki}$ respectively as:

$$e_{q,ki} = \frac{1}{\bar{\tau}_{ki}}\left(q_{ki}^{\tau_{ki}} - q_{ki}\right), \quad y_{q,ki} = \dot{q}_{ki} \tag{20}$$

where the $\mathcal{L}_2$-induced norm of the time-varying operator mapping the above defined input $e_{q,ki}$ and output $y_{q,ki}$ is bounded by 1 (Lemma 3, in Appendix A).

(ii) Input/output definition for $R(\alpha_i^\tau)\sum_k c_{ki}$*:* Consider the rotation matrix $R_0 = R(\alpha_i)$ defined in (3), where α_i is the estimation of the rotation angle by (7) unaffected by time delays. Define the input $e_{R,i}$ and output $y_{R,i}$ as:

$$\begin{aligned} e_{R,i} &= \frac{1}{h_i}\left(R\left(\alpha_i^\tau\right)\sum_k c_{ki} - R_0\sum_k c_{ki}\right), \\ y_{R,i} &= \sum_k\sum_j\left(\bar{\tau}_{ki}e_{q,ki}^T c_{kj}^\perp - \bar{\tau}_{ji}e_{q,ji}^T c_{kj}^\perp\right) = 2\sum_k\left(\bar{\tau}_{ki}\sum_j c_{kj}^{\perp T}\right)e_{q,ki}. \end{aligned} \tag{21}$$

where the $\mathcal{L}_2$-induced norm of the time-varying operator mapping the above defined input $e_{R,i}$ and output $y_{R,i}$ is bounded by 1 (Lemma 4, in Appendix A).

From the above input definitions $e_{q,ki}$ and $e_{R,i}$, the following equivalences can be easily deduced:

$$\begin{aligned} q_{ki}^{\tau_{ki}} &= q_{ki}^{\tau_{ki}} + q_{ki} - q_{ki} = q_{ki} + \bar{\tau}_{ki}e_{q,ki}, \\ R(\alpha_i^\tau)\sum_k c_{ki} &= R(\alpha_i^\tau)\sum_k c_{ki} + (R_0 - R_0)\sum_k c_{ki} = R_0\sum_k c_{ki} + h_i e_{R,i}. \end{aligned} \tag{22}$$

Replacing the terms $q_{ki}^{\tau_{ki}}$ and $R(\alpha_i^\tau)\sum_k c_{ki}$ from (22) into (8) we obtain:

$$u_i = K_c \sum_k d_{ki}^\tau = K_c \left(\sum_k \underbrace{(q_{ki} - R_0 c_{ki})}_{d_{ki}} + \sum_k \bar{\tau}_{ki} e_{q,ki} - h_i e_{R,i} \right). \tag{23}$$

Thus, from the equivalences (22), the state-space model (9) can be rewritten as the interconnected system formed by:

$$\dot{q}_{ji} = K_c \left(\sum_k \left(f_j d_{kj} - f_i d_{ki} + f_j \bar{\tau}_{kj} e_{q,kj} - f_i \bar{\tau}_{ki} e_{q,ki} \right) - f_j h_j e_{R,j} + f_i h_i e_{R,i} \right), \tag{24}$$

with the outputs $y_{q,ki}$, $y_{R,i}$ defined in (20), (21), and the feedback interconnections:

$$e_{q,ki} = \Delta_q^{ki} \cdot y_{q,ki}, \quad e_{R,i} = \Delta_R^i \cdot y_{R,i}, \quad \Delta_q^{ki} = \begin{bmatrix} \delta_q^{ki} & 0 \\ 0 & \delta_q^{ki} \end{bmatrix}, \tag{25}$$

through the corresponding time-varying operator δ_q^{ki} and Δ_R^i mapping their respective inputs and outputs. Note from Lemmas 3 and 4, in Appendix A, that $|\delta_q^{ki}| < 1$ (and therefore $||\Delta_q^{ki}||_\infty \leq 1$), and $||\Delta_R^i||_\infty \leq 1,\ \forall k, i$.

Define the following augmented column vectors $\bar{q}, \bar{d}, \bar{e}_q, \bar{y}_q \in \mathcal{R}^{2\bar{N}}$, $\bar{N} = N(N-1)$, $\bar{e}_R \in \mathcal{R}^{2N}$ and $\bar{y}_R \in \mathcal{R}^N$:

$$\begin{aligned} &\bar{q} = U \cdot col\left([q_{ij}]_{N\times N}^T \right), \quad \bar{d} = U \cdot col\left([d_{ij}]_{N\times N}^T \right), \\ &\bar{e}_q = U \cdot col\left([e_{q,ij}]_{N\times N}^T \right), \quad \bar{y}_q = U \cdot col\left([y_{q,ij}]_{N\times N}^T \right), \\ &\bar{e}_R = \left[e_{R,1}^T, \ \cdots \ , e_{R,2}^T \ , \cdots \ , e_{R,N}^T \right]^T, \\ &\bar{y}_R = \left[y_{R,1}^T, \ \cdots \ , y_{R,2}^T \ , \cdots \ , y_{R,N}^T \right]^T, \end{aligned} \tag{26}$$

where $U = Q_3 \otimes I_2$ and $Q_3 = diag\left(\mathcal{I}_N^1, \cdots, \mathcal{I}_N^N \right)$.

With the augmented vectors (26), the equations (24) and (25) can be written in matrix form and using polytopic description as the interconnected

system model formed by:

$$\begin{cases} M: & \begin{cases} \dot{\bar{q}} = K_c \bar{A} \bar{d} + K_c \begin{bmatrix} \delta \bar{B}_q & \bar{B}_R \end{bmatrix} \begin{bmatrix} \bar{e}_q \\ \bar{e}_R \end{bmatrix}, \\ \begin{bmatrix} \bar{y}_q \\ \bar{y}_R \end{bmatrix} = \begin{bmatrix} K_c \bar{A} \\ 0_{N \times 2\bar{N}} \end{bmatrix} \bar{d} + \begin{bmatrix} \delta K_c \bar{B}_q & K_c \bar{B}_R \\ \delta \bar{D} & 0_{N \times 2N} \end{bmatrix} \begin{bmatrix} \bar{e}_q \\ \bar{e}_R \end{bmatrix} \end{cases} \\ \Delta: & \begin{bmatrix} \bar{e}_q \\ \bar{e}_R \end{bmatrix} = \begin{bmatrix} \bar{\Delta}_q & 0 \\ 0 & \bar{\Delta}_R \end{bmatrix} \begin{bmatrix} \bar{y}_q \\ \bar{y}_R \end{bmatrix}, \end{cases} \tag{27}$$

where

$$\begin{aligned} &\bar{\Delta}_q = diag\left(\Delta_q^1, \cdots, \Delta_q^N\right), \quad \Delta_q^i = diag_{j=1, j\neq i}^N \left(\Delta_q^{ji}\right) \\ &\bar{\Delta}_R = diag\left(\Delta_R^1, \cdots, \Delta_R^N\right). \end{aligned} \tag{28}$$

and $\left(\bar{A}, \bar{B}_q, \bar{B}_R\right) = \sum_{f=1}^{2^{n_f}} \lambda_f(t) \left(\hat{\bar{A}}_f, \hat{\bar{B}}_{q,f}, \hat{\bar{B}}_{R,f}\right)$. Taking into account that some of the elements q_{ki} of the augmented vector $\bar{q}$ are linearly dependent, it is possible to obtain an equivalent reduced state-space realization of system (27) by defining the vectors $q_s, d_s \in \mathcal{R}^{2N-2}$ in (16) with linearly independent entries. Through the matrix $\mathcal{T}$ defined in (18) and its left inverse $\mathcal{T}^+ = \begin{bmatrix} I_{2N-2} & 0 \end{bmatrix}$, we can write $\bar{q} = \mathcal{T} q_s$, $\bar{d} = \mathcal{T} d_s$ and $q_s = \mathcal{T}^+ \bar{q}$, $d_s = \mathcal{T}^+ \bar{d}$. Then, replacing $\bar{q} = \mathcal{T} q_s$ and $\bar{d} = \mathcal{T} q_s$ into (27) we obtain:

$$M: \begin{cases} \mathcal{T} \dot{q}_s = K_c \bar{A} \mathcal{T} d_s + K_c \begin{bmatrix} \delta \bar{B}_q & \bar{B}_R \end{bmatrix} \begin{bmatrix} \bar{e}_q \\ \bar{e}_R \end{bmatrix}, \\ \begin{bmatrix} \bar{y}_q \\ \bar{y}_R \end{bmatrix} = \underbrace{\begin{bmatrix} K_c \bar{A} \mathcal{T} \\ 0_{N \times 2\bar{N}} \end{bmatrix}}_{L_K \mathcal{C}_s} d_s + \underbrace{\begin{bmatrix} \delta K_c \bar{B}_q & K_c \bar{B}_R \\ \delta \bar{D} & 0_{N \times 2N} \end{bmatrix}}_{L_K \mathcal{D}_s L_\delta} \begin{bmatrix} \bar{e}_q \\ \bar{e}_R \end{bmatrix} \end{cases}. \tag{29}$$

Pre-multiplying the first equation in (29) by $\mathcal{T}^+$ we have:

$$\dot{q}_s = K_c \underbrace{\mathcal{T}^+ \bar{A} \mathcal{T}}_{\mathcal{A}_s} d_s + K_c \underbrace{\mathcal{T}^+ \begin{bmatrix} \delta \bar{B}_q & \bar{B}_R \end{bmatrix}}_{\mathcal{B}_s L_\delta} \begin{bmatrix} \bar{e}_q \\ \bar{e}_R \end{bmatrix} \tag{30}$$

Finally, defining $e^T = \begin{bmatrix} \bar{e}_q^T & \bar{e}_R^T \end{bmatrix}$ and the unitary norm-bounded system $\Delta = \begin{bmatrix} \Delta_q & 0 \\ 0 & \Delta_R \end{bmatrix}$ (which embeds all the sources of time-varying uncertainties af-

fecting the relative position measurements and the rotation matrix), from (29) and (30) we obtain the interconnected system model (15). ■

4. Robust stability analysis

Small gain theorem (Theorem 1) can be applied to the interconnected system model (15) to find a sufficient condition to prove the robust exponential stability with decay-rate performance β (hereinafter, referred to as β-stability) of the formation control system (1) and (8):

Theorem 2 *Given positive scalars δ and K_c, if there exist scalars $\mu > 0, \xi_i > 0, i = 1, \cdots, N-1$, and symmetric matrices $S_i > 0$ ($S_i \in \mathcal{R}^2$), with $i = 1, \cdots, \bar{N}$ such that the following LMI are satisfied, $\forall f = 1, \cdots, 2^{n_f}$:*

$$\Omega_f < 0, \qquad \Omega_f = \begin{bmatrix} 2\mu K_c \hat{\mathcal{A}}_{s,f} + 2\beta\mu & \mu K_c \hat{\mathcal{B}}_{s,f} L_\delta & \hat{\mathcal{C}}_{s,f}^T L_K W_2 \\ (*) & -W_1 & L_\delta \hat{\mathcal{D}}_{s,f}^T L_K W_2 \\ (*) & (*) & -W_2 \end{bmatrix}, \quad (31)$$

being

$$W_1 = \begin{bmatrix} Z & \\ & X^* \end{bmatrix}, W_2 = \begin{bmatrix} Z & \\ & X \end{bmatrix}, Z = \begin{bmatrix} S_1 & & \\ & \cdots & \\ & & S_{\bar{N}} \end{bmatrix} \quad (32)$$

$$X^* = \begin{bmatrix} I_2 & & & \\ & \xi_1 I_2 & & \\ & & \cdots & \\ & & & \xi_{N-1} I_2 \end{bmatrix}, \; X = \begin{bmatrix} 1 & & & \\ & \xi_1 & & \\ & & \cdots & \\ & & & \xi_{N-1} \end{bmatrix}$$

and L_δ, L_K, $\hat{\mathcal{A}}_{s,f}, \hat{\mathcal{B}}_{s,f}, \hat{\mathcal{C}}_{s,f}, \hat{\mathcal{D}}_{s,f}$ defined in (16)*, then the interconnected system* (15) *is robustly β-stable. Therefore, the formation control system* (1)-(8) *converges to the desired configuration fulfilling $||d_s(t)|| \leq \mathcal{Q}_d ||d_s(0)|| e^{-\beta t}, \forall t \geq 0$ (for some positive constant $\mathcal{Q}_d$ and d_s defined in* (16)*), regardless of the value of time-varying delays satisfying $\tau_{ki}(t) \leq \delta \hat{\tau}_{ki}$ and actuator faults* (2)*.*

Proof: Note from (12) the following properties: $0 \leq \lambda_f(t) \leq 1, \; f = 1, ..., 2^{n_f}$ and $\sum_{f=1}^{2^{n_f}} \lambda_f(t) = 1, \; \forall t \geq 0$. Therefore, the fulfilment of the LMI in (31) is a sufficient condition for $\rho^T \left(\sum_{f=1}^{2^{n_f}} \lambda_f(t) \Omega_f \right) \rho < 0, \forall t \geq 0$ and any $\rho \neq 0$. From the definition of $\dot{q}_s$ in (30) and taking $\rho^T = \begin{bmatrix} \hat{d}^T & e^T \end{bmatrix}$, it can be deduced that (31) implies:

$$\mu d_s^T \dot{q}_s + \mu \dot{q}_s^T d_s + 2\beta\mu + y^T W_2 y - e^T W_1 e < 0 \quad (33)$$

From the fact that $W_1, W_2 > 0$, we can find T_1, T_2 such that $W_1 = T_1^T T_1$, $W_2 = T_2^T T_2$ and $T_1\Delta = \Delta T_2$, where Δ is defined in (15). To prove the stability of the interconnected system (15) (see Fig. 1), it suffices to prove that the fulfilment of (33) implies the two conditions given in Theorem 1: (i) the internal β-stability of system M, and (ii) the condition $||T_2 M T_1^{-1}||_\infty < 1$:

(i) Proof of the internal β-stability of system M: consider the Lyapunov function candidate:

$$V = \mu \, ||d_s||^2 > 0 \tag{34}$$

where μ is a positive scalar and d_s is defined in (16). The time derivative $\dot{V}$ yields:

$$\dot{V} = \frac{\partial V}{\partial d_s}\dot{d}_s + \frac{\partial V}{\partial \alpha}\dot{\alpha} \tag{35}$$

where α is the rotation angle of the desired target formation (5), unaffected by delays. From the fact that $V = \mu J$, where $J \equiv J_i$ is the cost function (4), we deduce that $\frac{\partial V}{\partial \alpha} = 0$ and therefore:

$$\dot{V} = \frac{\partial V}{\partial d_s}\dot{d}_s = \mu d_s^T \dot{q}_s + \mu \dot{q}_s^T d_s \tag{36}$$

From (36), the inequality (33) can be also written as:

$$\dot{V} + 2\beta V + y^T W_2 y - e^T W_1 e < 0 \tag{37}$$

To prove the internal β-stability of system M, we need to guarantee the fulfilment of the Lyapunov stability criterion $\dot{V} + 2\beta V < 0, \ \forall \hat{d}$ with zero input $e = 0$. From (37), if we set $e = 0$ we have:

$$\dot{V} + 2\beta V + y^T W_2 y < 0 \tag{38}$$

As long as $W_2 > 0$, we have that (38) implies $\dot{V} + 2\beta V < 0$. In other words, the fulfilment of (31) implies the existence of a positive function V (34) satisfying the Lyapunov criterion for the internal stability of system M, along with the condition $||d_s(t)|| \leq \mathcal{Q}_d ||d_s(0)|| e^{-\beta t}, \forall t \geq 0$, for some positive constant $\mathcal{Q}_d$.

(ii) Proof of the condition $||T_2 M T_1^{-1}||_\infty < 1$: By integrating the inequality (37) we obtain:

$$V(\infty) - V(0) + 2\beta \int_0^\infty V(t)dt + \int_0^\infty \left(y^T W_2 y - e^T W_1 e\right) dt < 0 \tag{39}$$

With the aim to verify $||T_2 M T_1^{-1}||_\infty < 1$, by virtue of Definition 2, we have to consider zero state initial conditions for system M. Therefore, we set $\hat{d}(0) = 0$ and, from (34), we obtain $V(0) = 0$. Then, (39) yields:

$$V(\infty) + 2\beta \int_0^\infty V(t)dt < \int_0^\infty \left(-y^T W_2 y + e^T W_1 e\right) dt \tag{40}$$

If (31) is fulfilled, we have that $V > 0$ exists. Also, taking into account that β are always positive, we obtain from (40) that:

$$\int_0^\infty \left(-y^T W_2 y + e^T W_1 e\right) dt > 0 \tag{41}$$

and therefore:

$$\int_0^\infty y^T W_2 y \; dt < \int_0^\infty e^T W_1 e \; dt \tag{42}$$

Finally, from Definition 2 and $W_1 = T_1^T T_1$, $W_2 = T_2^T T_2$, the inequality (42) implies the fulfilment of:

$$||T_2 M T_1^{-1}||_\infty < 1 \tag{43}$$

■

If δ is sufficiently small, the following corollary demonstrates that the formation control system is exponentially stable with decay rate β, provided that M in (15) is internally β-stable:

Corollary 1 *Given a sufficiently small worst-case point-to-point delay $\delta > 0$, the formation control system* (1)-(8) *exponentially converges to the desired target formation with decay rate β if the system M in* (15) *is internally β-stable.*

Proof: Let $T_1 = diag(I_{2\bar{N}}, \frac{1}{\sqrt{\delta}} I_{2N})$ and $T_2 = diag(I_{2\bar{N}}, \frac{1}{\sqrt{\delta}} I_N)$. The system $M^* = T_2 M T_1^{-1}$, where M is defined in (15), renders:

$$M^* = \left[\begin{array}{c|c} K_c \mathcal{A}_s & K_c \mathcal{B}_s L_\delta T_1 \\ \hline T_2^{-1} L_K \mathcal{C}_s & T_2^{-1} L_K \mathcal{D}_s L_\delta T_1 \end{array}\right] = \left[\begin{array}{c|c} K_c \mathcal{A}_s & K_c \mathcal{B}_s^* \\ \hline L_K \mathcal{C}_s & L_K \mathcal{D}_s^* \end{array}\right], \tag{44}$$

where:

$$\mathcal{B}_s^* = \mathcal{T}^+ \sum_{f=1}^{2^{n_f}} \lambda_f(t) \left[\delta \hat{\bar{B}}_{q,f} \qquad \sqrt{\delta} \hat{\bar{B}}_{R,f}\right], \quad \mathcal{B}_s^* = \sum_{f=1}^{2^{n_f}} \lambda_f(t) \begin{bmatrix} \delta \hat{\bar{B}}_{q,f} & \sqrt{\delta} \hat{\bar{B}}_{R,f} \\ \sqrt{\delta} \bar{D} & 0_{N \times 2N} \end{bmatrix} \tag{45}$$

From (45) it can be seen that $\mathcal{B}_s^*$ and $\mathcal{D}_s^*$ vanish when the worst-case point-to-point delay $\delta \to 0$, leading to $||M^*||_\infty \to 0$ and therefore the fulfilment of $||T_2 M T_1^{-1}||_\infty < 1$ for δ small enough. In such case, the formation control system (1)-(8) will be β-stable, provided that the system M is internally β-stable (condition (i) in the proof of Theorem 2). ■

Note that the internal stability of M is achieved by properly choosing the control gain K_c in (8). In absence of actuator faults and time delays, it is sufficient to choose $K_c > 0$ for stability, (or $K_c > \beta/N$ for β-stability) [14].

From Theorem 2 and Corollary 1, we propose the following algorithm to easily obtain the maximum worst-case point-to-point delay δ, given β and K_c, where $\epsilon_\delta > 0$ is the prespecified error tolerance on the estimation of δ:

Algorithm 1

- *(i) Set $k = 0$ and some $\Delta_\delta > 0$. Choose the initial value of the worst-case point-to-point delay $\delta^{(0)}$ sufficiently small to obtain a feasible solution for LMI* (31) [2].
- *(ii) Set $\delta^{(k+1)} = \delta^{(k)} + \Delta_\delta$, $k + 1 := k$, and solve LMI* (31).
- *(iii) If a feasible solution exists for LMI* (31)*, go to step (ii). Otherwise, set $\Delta_\delta = \gamma \Delta_\delta$, for some $0 < \gamma \leq 1$, and go to step (iv).*
- *(iv) If $\Delta_\delta \leq \epsilon_\delta$ stop. Otherwise, go to step (ii).*

Remark 2 *The control gain K_c can be adjusted by means of Algorithm 1 and line search on K_c to improve robust performance, given a prescribed decay rate β. On the one hand, if we set $K_c = \beta/N + \epsilon$ with ϵ small, the closed-loop pole is very close to the limit of β-stability, taking into account that $\beta = K_c N$ in absence of delays and actuator faults [14]. Therefore, small perturbations might lead the system to instability (if $\beta = 0$), or not fulfilment of the decay rate performance criterion (if $\beta > 0$). On the other hand, the robustness against time delays decreases when K_c grows. Therefore, it is expected that there will be some $K_c > \beta/N$ which gives the best performance in terms of robustness against time delays. Based on this fact, the control gain K_c can be*

[2] By virtue of Corollary 1, a feasible solution for LMI (31) always exists for a sufficiently small δ.

adjusted by Algorithm 1 and line search by increasing K_c starting from some initial value slightly greater than β/N.

Remark 3 *One of the advantages of allowing arbitrarily fast time-varying delays is that sampling-based sensors with zero-order hold mechanisms can be taken into account. Indeed, the relationship between the transmitted measurement and the resulting piecewise-constant data obtained from acquiring the measurement at sampling instants $t_h,\ (h = 0, 1, \cdots)$ and holding its value during the inter-sample time period can be modeled through time delays of sawtooth structure with positive unitary slope and discontinuities at each t_h, that is, $\tau(t) = t - t_h,\ t \in [t_h,\ t_{h+1})$. Such discontinuities imply that its time-derivative $\dot{\tau}(t)$ cannot be bounded. Therefore, our method can be applied to systems in which sampling-based sensors are implemented, and the following condition can be easily deduced: $t_{h+1} - t_h \leq \delta - max(\tau_{ki}(t)), \forall k, i \in [1, ..., N] \times [1, ..., N],\ \forall h \geq 0, \forall t \geq 0$, where $t_{h+1} - t_h$ is the sampling period and $max(\tau_{ki}(t))$ is the maximum communication delay value.*

Remark 4 *Regarding computational complexity aspects, LMI can be efficiently solved by means of semidefinite-programming tools [34]. Indeed, efficient polynomial-time optimization algorithms (e.g., interior-point [37]) are available in standard commercial libraries, such as the LMI Control Toolbox [38] and SEDUMI [39]. Nevertheless, the number of decision variables (NoV) and the size of LMI in* (31) *are related with the number of agents N as $3N(N-1)+N$ and $2(N-1)+4N(N-1)+3N$ respectively, which clearly imposes numerical load limitations for large systems. To alleviate this drawback, one can set $S_i = S$ and $\xi_i = \xi$ in* (31) *leading to $NoV = 5$ regardless N, but at the expense of additional conservatism due to the inherent loss of generality. The reduction on complexity of the given algorithm for large systems is pointed out as a matter of future research.*

Remark 5 *Note that the parameter H defined in Assumption 1 plays a key role to find an upper bound for the nonlinear term through the inequality* (52) *in the proof of Theorem 2. In absence of time delays, one of the following*

two conditions:

$$(i) \quad \frac{1}{p}\left|\sum_k \sum_j q_{kj}^T(t=0)c_{kj}\right| \leq |\sum_k \sum_j q_{kj}^T c_{kj}| \leq p \sum_k \sum_j ||c_{kj}||^2, \qquad (46)$$

$$(ii) \quad \frac{1}{p}\sum_k \sum_j ||c_{kj}||^2 \leq |\sum_k \sum_j q_{kj}^T c_{kj}| \leq p\left|\sum_k \sum_j q_{kj}^T(t=0)c_{kj}\right|$$

always holds for any $p \geq 1$, taking into account that $lim_{t\to\infty} q_{kj}(t) = c_{kj}$. Nevertheless, this condition is not necessarily satisfied taking $p = 1$ when time delays appear, because of the perturbations on the agents' trajectories. Therefore, the security factor p should be chosen to be high enough to ensure (46) *in presence of time delays. However, the larger p is chosen, the more conservative will be the estimated worst-case point-to-point delay δ by Algorithm 1 and Theorem 2. In practice, the choice $p = 2$ is a good trade-off between security and conservativeness [14], leading to Assumption 1 by only combining the left-side inequalities (i) and (ii) given in* (46)*.*

5. Simulations

In this section, simulation results are provided to show the robust performance of the coordinate-free formation control system in presence of time-varying delays and actuator faults. For all the performed simulations, each time-varying delay pattern $\tau_{ki} \equiv \tau_{ki}(t)$ is randomly generated with values between $[0, \bar{\tau}_{ki}]$. For simplicity, the upper bound for each τ_{ki} is chosen to be equal to the worst-case point-to-point delay: $\bar{\tau}_{ki} = \delta,\ \forall k, i$, obtaining all the normalized upper bound delays $\hat{\tau}_{ki} = 1$ ($\hat{\tau}_{ki}$ are introduced in Definition 1).

Simulation 1. Let us consider the following three target formations depicted in Fig. 2, with number of agents $N = 4, 6, 8$ respectively. The idea is to maximize the worst-case point-to-point delay δ by adjusting K_c so that the exponential stability with decay rate $\beta = 0.01$ is achieved (which leads to a 5% settling time of around 300s). The following two cases are considered:

(i) No actuator faults: By means of Algorithm 1 and line search on K_c (following Remark 2), we find the following values of K_c which give the maximum δ (see Table 1, left-side). The parameters chosen for Algorithm 1 are $\gamma = 0.5$, $\delta^{(0)} = 0.1s$ and $\epsilon_\delta = 0.1s$. The parameter H (which is necessary to check LMI (31) by building $\hat{\mathcal{B}}_{s,f}$ from (16),(18) and (19)) is obtained from Assumption 1 for each target formation given in Fig. 2. With the aim

to cover a wide set of possible initial conditions for the relative interagent positions $q_{ki}(t=0)$, we have taken the most unfavorable case from a large set of possible values for such initial conditions, chosen randomly with maximum interagent distance of $50m$. The obtained values are $H = 257,\ 638,\ 930$ for $N = 4, 6, 8$ with target formations in Fig. 2, respectively.

It is worthwhile to compare with the worst-case point-to-point delay in [14] through the expression: $\frac{1}{2(1+B)K_eK_c(N-1)\sqrt{N}}$, where $K_e = 1 + (4(N-1)max_{k,i}||c_{ki}||\ max_i||\sum_k c_{ki}||)/H$. The parameter H is the same as Assumption 1, and B comes from [14, Assumption A2]. The parameter B must be obtained from the boundedness of the disturbance created by time delays. The avoidance of this last assumption is pointed out as one of our contributions, along with the extension to time-varying delays. Moreover, it can be seen from Table 2 that less conservative estimation of the worst-case point-to-point delay is achieved through our method, even by considering a very *optimistic* worst-case delay estimation through the expression given in [14] (see above), by intentionally taking a small value for B of 10^{-3}. For a fair comparison, the same values for H and K_c have been considered at each case.

On the other hand, note from Fig. 3 (left-side) the existence of a value for K_c which maximizes δ, as discussed in Remark 2. Simulation results are depicted on Fig. 5 (left-side) for the hexagonal target formation given in Fig. 2 with $N = 6$. It can be seen that the system converges to the desired formation, as theoretically expected, when $K_c = 4.1 \cdot 10^{-3}$ and all time-varying delays τ_{ki} are bounded by $\delta = 10.8s$.

(ii) Actuator faults: Let the agents 1 and 3 be subject to actuator faults modeled by (2) with $\underline{f}_1 = 0.3$, $\underline{f}_3 = 0.1$, $\overline{f}_1 = 1$, $\overline{f}_3 = 1$. In this case, by Algorithm 1 (considering the same values for γ, $\delta^{(0)}$ and ϵ_δ) and line search on K_c we obtain the values depicted on Table 1 (right-side) for the control gain K_c maximizing δ for each case. For simulation purposes, we consider the hexagonal target formation given in Fig. 2 with $N = 6$, and the actuator faults $f_1(t)$ and $f_3(t)$ (see Fig. 4), corresponding to the agents 1 and 3 respectively. Simulation results are depicted on Fig. 5 (right-side): it can be seen that the system converges to the desired formation, as theoretically expected, when $K_c = 21.7 \cdot 10^{-3}$ and all time-varying delays τ_{ki} are bounded by $\delta = 1.4s$.

In both cases, the trajectories followed by each agent and their estimation of the rotation angle α_i are respectively displayed in the first and second rows of Fig. 5. Note that the velocity norm of each agent (third row on Fig 5)

N	No actuator faults	Actuator faults
4	$K_c = 5.0 \cdot 10^{-3}$ $(\delta = 11.0s)$	$K_c = 26.5 \cdot 10^{-3}$ $(\delta = 1.8s)$
6	$K_c = 4.1 \cdot 10^{-3}$ $(\delta = 10.8s)$	$K_c = 21.7 \cdot 10^{-3}$ $(\delta = 1.4s)$
8	$K_c = 3.8 \cdot 10^{-3}$ $(\delta = \ 8.1s)$	$K_c = 16.3 \cdot 10^{-3}$ $(\delta = 1.0s)$

Table 1: Maximum worst-case point-to-point delay δ for each target formation in Fig. 2. The control gain K_c has been adjusted by Algorithm 1 and line search on K_c. Left-side, no actuator faults; Right-side, actuator faults in agents 1 and 3, modeled by (2) with $\underline{f}_1 = 0.3$, $\underline{f}_3 = 0.1$, $\overline{f}_1 = 1$, $\overline{f}_3 = 1$.

N	K_c	δ (Algorithm 1)	δ [14] - for time-constant delays
4	$5.0 \cdot 10^{-3}$	11.0s	0.24s
6	$4.1 \cdot 10^{-3}$	10.8s	0.11s
8	$3.8 \cdot 10^{-3}$	8.1s	0.05s

Table 2: Comparison of the worst-case point-to-point delay δ obtained by Algorithm 1 with the obtained by [14] for time-constant delays. Target formations are depicted in Fig. 2

vanishes when the convergence to the target formation is reached. Note also that the normalized cost function $J(t)/J(0)$ (continuous line) is always below the theoretical bound $e^{-2\beta t}$ (dashed line) with $\beta = 0.01$ (fourth row on Fig. 5). This confirms the exponential asymptotic convergence of the cost function $J(t)$ with $\beta = 0.01$, even in presence of time-varying delays $\tau_{ki} \leq \delta$, $\forall k, i$ and actuator faults.

Simulation 2. Consider a 4×3 rectangular formation composed by $N = 12$ agents, where the distance between agents is $6m$ both in X and Y axes. Let the agents 1 and 11 be subject to actuator faults modeled by (2) with $\underline{f}_1 = 0.2$, $\underline{f}_{11} = 0.2$, $\overline{f}_1 = 1$, $\overline{f}_{11} = 1$. Also, let us consider a prescribed decay rate $\beta = 0.01$. By Algorithm 1 and line search on K_c, we obtain the

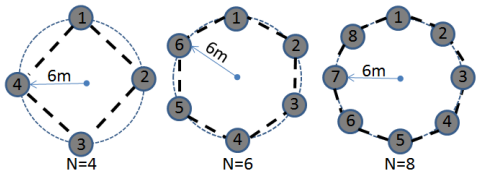

Figure 2: Different target formations for the three cases under analysis with number of agents: N=4, N=6 and N=8 respectively.

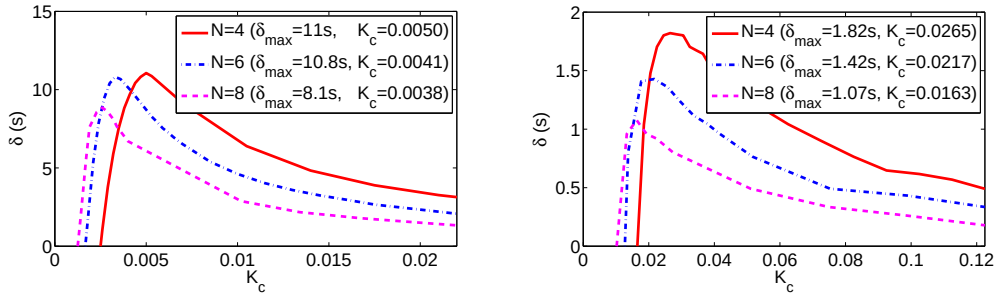

Figure 3: Worst case point-to-point delay δ (in seconds) obtained from Algorithm 1 for different values of K_c and the target formations depicted in Fig. 2 for $N = 4, 6$ and 8 respectively. Left-side, no actuators faults; Right-side, with actuator faults in agents 1 and 3.

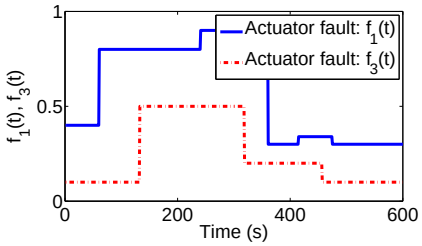

Figure 4: Actuator faults $f_1(t)$ and $f_3(t)$ (see (2)) on agents 1 and 3 for the hexagonal target formation depicted in Fig. 2 ($N = 6$).

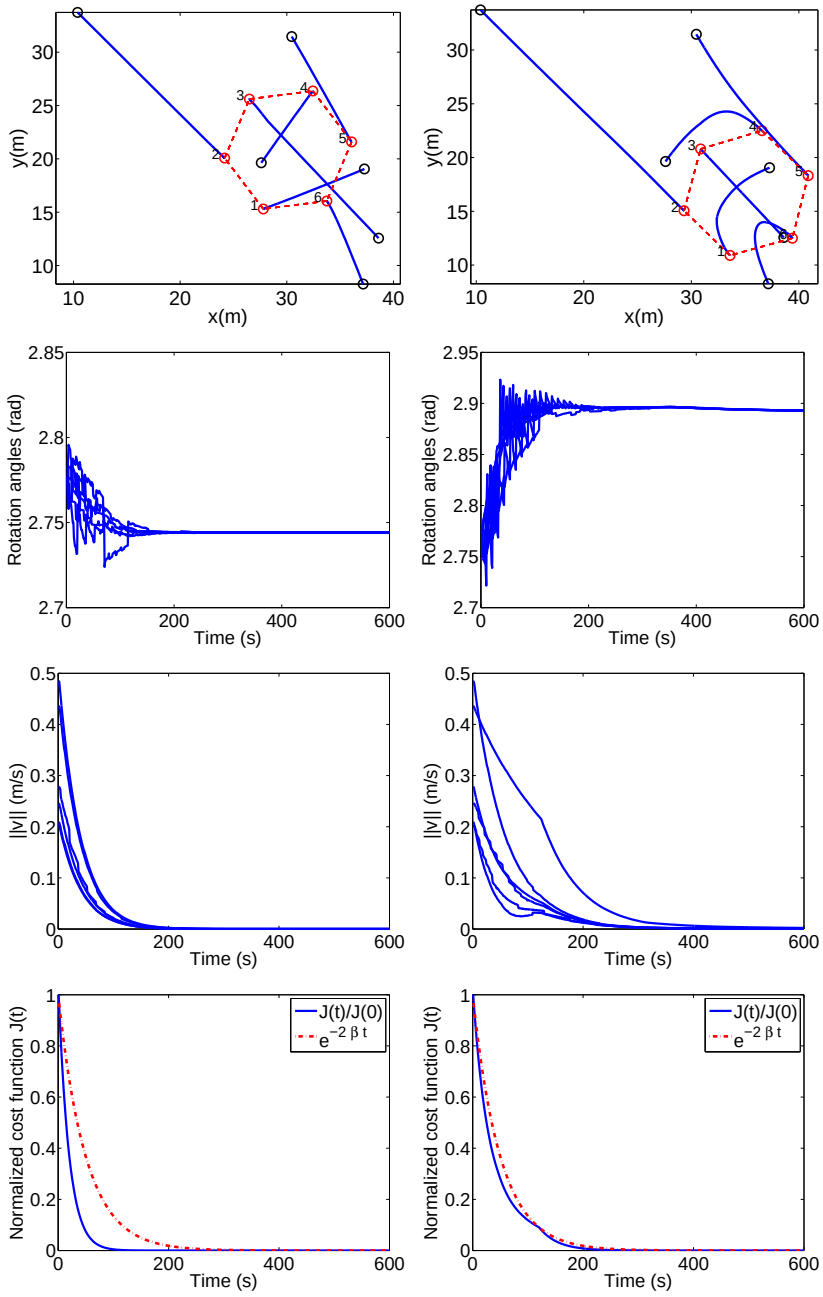

Figure 5: Formation control of hexagonal formation pattern $N = 6$ and time-varying communication delays bounded by δ: left-side: no actuator faults, right-side: actuator faults given in Fig. (4) for agents 1 and 3. First row: trajectories followed by each agent. Second row: estimation of the rotation angle α_i made by each agent. Third row: velocitiy norm of each agent. Last row, comparison of the normalized cost function $J(t)/J(0)$ with the theoretical bound $e^{-2\beta t}$, where $\beta = 0.01$ is the prescribed decay rate.

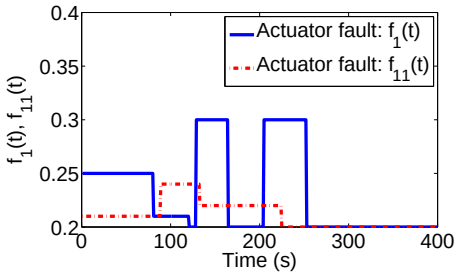

Figure 6: Actuator faults $f_1(t)$ and $f_{11}(t)$ (see (2)) on agents 1 and 11 for the 4×3 rectangular target formation with $N = 12$.

control gain $K_c = 10^{-2}$ which maximizes $\delta = 1s$. The parameters chosen for Algorithm 1 are $\gamma = 0.5$, $\delta^{(0)} = 0.1s$ and $\epsilon_\delta = 0.1s$. The parameter H has been obtained following the same criterion as in Simulation 1, and renders $H = 5538$.

For simulation purposes, we consider the actuator faults $f_1(t)$ and $f_{11}(t)$ (corresponding to the agents 1 and 11 respectively) such as depicted in Fig. 6. Simulation results are displayed in Fig. 7, in which it can be seen that the system exponentially converges to the desired formation, as theoretically expected.

6. Conclusions and perspectives

We have presented a sufficient condition based on LMI to ensure the robust asymptotic convergence of coordinate-free multiagent formation control systems subject to time-varying delays and actuator faults, given an upper bound for the worst-case point-to-point delay. In this application, the proposed method generalizes with respect to previously reported approaches in three aspects: (i) it deals with arbitrarily fast time-varying delays, (ii) prior knowledge of the boundedness of the disturbance created by time delays is not required and (iii), actuator faults are considered. Moreover, the estimation may be less conservative than other existing similar results, as illustrated through some simulation examples. Future developments could address how to alleviate some practical limitations by, e.g., guaranteeing the maintenance of connectivity and the absence of collisions during control, or improving the trade-off between complexity on the given algorithms and conservatism on the estimated maximum worst-case point-to-point delay. In addition, allowing incomplete interaction topologies would avoid overloading the agents'

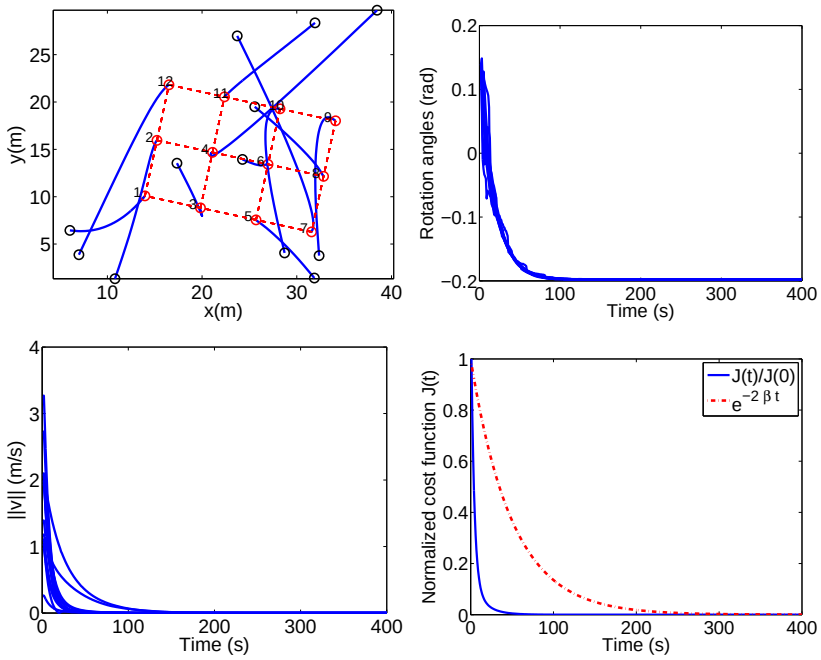

Figure 7: Rectangular 4×3 formation control ($N = 12$ agents) with random time-varying communication delays τ_{ki} bounded by $\delta = 1.02s$ and actuator faults given in Fig. (6) for agents 1 and 11: Upper-left: trajectories followed by each agent converging to the desired geometric configuration; upper-right: estimation of the rotation angle α_i made by each agent; lower-left: velocitiy norm of each agent; lower-right: normalized cost function vs decay-rate $e^{-2\beta t}$ with $\beta = 0.01$.

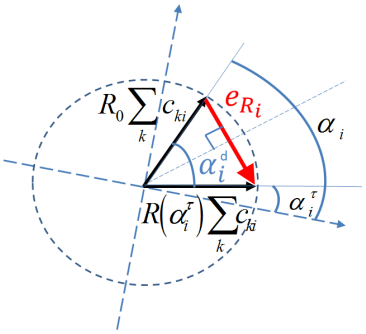

Figure 8: Representation of the error vector $e_{R,i}$ due to time-varying delays. The variables are expressed in an arbitrary global frame.

resources in the case of very large networks.

Acknowledgement

This work was supported by French Government research program Investissements d'avenir through the RobotEx Equipment of Excellence (ANR-10-EQPX-44) and the LabEx IMobS3 (ANR7107LABX716701), and by Spanish Government/European Union Project DPI2015-69376-R (MINECO/FEDER).

Apppendix A

Lemma 3 *The $\mathcal{L}_2$-induced norm of the time-varying operator mapping the input $e_{q,ki}$ in (20) and the output $y_{q,ki} = \dot{q}_{ki}$ in (20) is bounded by 1, $\forall t \geq 0$.*

Proof: From the definition of $e_{q,ki}$ in (20), it can be easily deduced that:

$$e_{q,ki} = -\frac{1}{\bar{\tau}_{ki}} \int_{t-\tau_{ki}(t)}^{t} \dot{q}_{ki}(t)dt \tag{47}$$

The rest of the proof can be outlined from Lemma 1. ■

Lemma 4 *The $\mathcal{L}_2$-induced norm of the time-varying operator mapping the input $e_{R,i}$ in (21) and the output $y_{R,i}$ in (21) is bounded by 1, $\forall t \geq 0$.*

Proof: From Fig. 8, applying trigonometry it can be proved that:

$$\left|\left| R\left(\alpha_i^\tau\right) \sum_k c_{ki} - R_0 \sum_k c_{ki} \right|\right| = 2\left|sin(\alpha_{d,i}/2)\right| \left|\left| \sum_k c_{ki} \right|\right| \tag{48}$$

where $\alpha_{d,i}$ is the difference between the rotation angles encapsulated by $R(\alpha_i)$ and $R(\alpha_i^\tau)$. From the definition of $e_{R,i}$ in (21), multiplying both sides of (48) by $1/h_i$ and squaring, we have:

$$||e_{R,i}||^2 = \frac{4}{h_i^2}|sin(\alpha_{d,i}/2)|^2 \left|\left|\sum_k c_{ki}\right|\right|^2 \tag{49}$$

Taking into account that $|sin(\alpha_{d,i}/2)| \leq |tan(\alpha_{d,i})|/2$, from (49) the following inequality can be deduced:

$$||e_{R,i}||^2 \leq \frac{1}{h_i^2}|tan(\alpha_{d,i})|^2 \left|\left|\sum_k c_{ki}\right|\right|^2 \tag{50}$$

On the other hand, noticing from (20) that $\bar{\tau}_{kj}e_{q,kj} = q_{kj}^{\tau_{kj}} - q_{kj}$, we can write (7) as:

$$|tan(\alpha_{d,i})| = \frac{\left|\sum_k \sum_j \left(\left(\bar{\tau}_{ki}e_{q,ki}^T - \bar{\tau}_{ji}e_{q,ji}^T\right) c_{kj}^\perp\right)\right|}{\left|\sum_k \sum_j \left(q_{kj}^{*T} c_{kj}\right)\right|}, \tag{51}$$

where $q_{kj}^{*T} = \left(q_{ki}^{\tau_{ki}} - q_{ji}^{\tau_{ji}}\right)^T$ is equivalent to the delayed q_{kj}. From Assumption 1 and the above expression, we have:

$$|tan(\alpha_{d,i})| \leq \frac{\left|\sum_k \sum_j \left(\bar{\tau}_{ki}e_{q,ki}^T c_{kj}^\perp - \bar{\tau}_{ji}e_{q,ji}^T c_{kj}^\perp\right)\right|}{H} \tag{52}$$

Therefore, combining the inequalities (52) and (50), and applying the definition of $y_{R,i}$ in (21), we obtain:

$$||e_{R,i}||^2 \leq \frac{1}{h_i^2 H^2}\left|\left|\sum_k c_{ki}\right|\right|^2 ||y_{R,i}||^2$$

From the definition of h_i in (19) the above inequality can be simplified as:

$$||e_{R,i}||^2 \leq ||y_{R,i}||^2 \tag{53}$$

Therefore, the $\mathcal{L}_2$ norm of $e_{R,i}$ can be bounded as follows:

$$||e_{R,i}||_2^2 = \int_0^\infty ||e_{R,i}||^2 dt \leq \int_0^\infty ||y_{R,i}||^2 dt = ||y_{R,i}||_2^2 \tag{54}$$

Finally, applying Definition 2, it is proved that the $\mathcal{L}_2$-induced norm of the time-varying operator mapping $e_{R,i}$ to $y_{R,i}$ is bounded by 1. ■

References

[1] W. Ren, E. Atkins, Distributed multi-vehicle coordinated control via local information exchange, International Journal of Robust and Nonlinear Control 17 (10-11) (2007) 1002–1033.

[2] J. Alonso-Mora, M. Schoch, A. Breitenmoser, R. Siegwart, P. Beardsley, Object and animation display with multiple aerial vehicles, in: IEEE/RSJ International Conference on Intelligent Robots and Systems, 2012, pp. 1078–1083.

[3] D. Tardioli, D. Sicignano, L. Riazuelo, A. Romeo, J. L. Villarroel, L. Montano, Robot teams for intervention in confined and structured environments, Journal of Field Robotics 33 (6) (2015) 765–801.

[4] J. Ghommam, M. S. Mahmoud, M. Saad, Robust cooperative control for a group of mobile robots with quantized information exchange, Journal of the Franklin Institute 350 (8) (2013) 2291–2321.

[5] K.-K. Oh, M.-C. Park, H.-S. Ahn, A survey of multi-agent formation control, Automatica 53 (2015) 424–440.

[6] M. M. Zavlanos, G. J. Pappas, Distributed formation control with permutation symmetries, in: 46th IEEE Conference on Decision and Control, 2007, pp. 2894–2899.

[7] L. Sabattini, C. Secchi, C. Fantuzzi, Arbitrarily shaped formations of mobile robots: artificial potential fields and coordinate transformation, Autonomous Robots 30 (4) (2011) 385–397.

[8] K.-K. Oh, H.-S. Ahn, Formation control of mobile agents based on inter-agent distance dynamics, Automatica 47 (10) (2011) 2306–2312.

[9] D. V. Dimarogonas, K. J. Kyriakopoulos, A connection between formation infeasibility and velocity alignment in kinematic multi-agent systems, Automatica 44 (10) (2008) 2648–2654.

[10] S. Coogan, M. Arcak, Scaling the size of a formation using relative position feedback, Automatica 48 (10) (2012) 2677–2685.

[11] K.-K. Oh, H.-S. Ahn, Formation control and network localization via orientation alignment, IEEE Transactions on Automatic Control 59 (2) (2014) 540–545.

[12] L. Krick, M. E. Broucke, B. A. Francis, Stabilisation of infinitesimally rigid formations of multi-robot networks, International Journal of Control 82 (3) (2009) 423–439.

[13] Y.-P. Tian, Q. Wang, Global stabilization of rigid formations in the plane, Automatica 49 (5) (2013) 1436–1441.

[14] M. Aranda, G. López-Nicolás, C. Sagüés, M. M. Zavlanos, Coordinate-free formation stabilization based on relative position measurements, Automatica 57 (2015) 11–20.

[15] K. Gu, J. Chen, V. L. Kharitonov, Stability of time-delay systems, Springer Science & Business Media, 2003.

[16] J.-P. Richard, Time-delay systems: an overview of some recent advances and open problems, Automatica 39 (10) (2003) 1667–1694.

[17] S. Knorn, Z. Chen, R. H. Middleton, Overview: Collective control of multiagent systems, IEEE Transactions on Control of Network Systems 3 (4) (2016) 334–347.

[18] Z. Kan, T. Yucelen, E. Doucette, E. Pasiliao, A finite-time consensus framework over time-varying graph topologies with temporal constraints, Journal of Dynamic Systems, Measurement, and Control 139 (7) (2017) 7–12.

[19] H. Liu, H. R. Karimi, S. Du, W. Xia, C. Zhong, Leader-following consensus of discrete-time multiagent systems with time-varying delay based on large delay theory, Information Sciences 417 (2017) 236 – 246.

[20] Y. Tang, X. Xing, H. R. Karimi, L. Kocarev, J. Kurths, Tracking control of networked multi-agent systems under new characterizations of impulses and its applications in robotic systems, IEEE Transactions on Industrial Electronics 63 (2) (2016) 1299–1307.

[21] S. Rathinasamy, H. R. Karimi, M. Joby, S. Santra, Resilient sampled-data control for markovian jump systems with an adaptive fault-tolerant

mechanism, IEEE Transactions on Circuits and Systems II: Express Briefs 64 (11) (2017) 1312–1316.

[22] Y. Wei, J. Qiu, H. R. Karimi, Reliable output feedback control of discrete-time fuzzy affine systems with actuator faults, IEEE Transactions on Circuits and Systems I: Regular Papers 64 (1) (2017) 170–181.

[23] X.-J. Wei, Z.-J. Wu, H. R. Karimi, Disturbance observer-based disturbance attenuation control for a class of stochastic systems, Automatica 63 (2016) 21–25.

[24] J. Nilsson, Real-time control systems with delays, Ph.D. dissertation, Department of Automatic Control, Lund Institute of Technology, 1998.

[25] E. Fridman, New lyapunov–krasovskii functionals for stability of linear retarded and neutral type systems, Systems & Control Letters 43 (4) (2001) 309–319.

[26] A. Gonzalez, T. Guerra, An improved robust stabilization method for discrete-time fuzzy systems with time-varying delays, Journal of the Franklin Institute 351 (11) (2014) 5148–5161.

[27] X. Li, H. Gao, A new model transformation of discrete-time systems with time-varying delay and its application to stability analysis, IEEE Transactions on Automatic Control 56 (9) (2011) 2172–2178.

[28] A. González, A. Sala, R. Sanchis, Lk stability analysis of predictor-based controllers for discrete-time systems with time-varying actuator delay, Systems & Control Letters 62 (9) (2013) 764–769.

[29] Z. Wu, H. R. Karimi, P. Shi, Dissipativity-based small-gain theorems for stochastic network systems, IEEE Transactions on Automatic Control 61 (8) (2016) 2065–2078.

[30] L. Han, X. Dong, Q. Li, Z. Ren, Formation-containment control for second-order multi-agent systems with time-varying delays, Neurocomputing 218 (2016) 439–447.

[31] D. Xue, J. Yao, J. Wang, Y. Guo, X. Han, Formation control of multi-agent systems with stochastic switching topology and time-varying communication delays, IET Control Theory & Applications 7 (13) (2013) 1689–1698.

[32] X. Dong, Q. Li, Z. Ren, Y. Zhong, Formation-containment control for high-order linear time-invariant multi-agent systems with time delays, Journal of the Franklin Institute 352 (9) (2015) 3564–3584.

[33] A. Papachristodoulou, A. Jadbabaie, U. Münz, Effects of delay in multi-agent consensus and oscillator synchronization, IEEE Transactions on Automatic Control 55 (6) (2010) 1471–1477.

[34] S. Boyd, L. El Ghaoui, E. Feron, V. Balakrishnan, Linear matrix inequalities in system and control theory, Philadelphia, P.A: SIAM, 1994.

[35] K. Zhou, J. C. Doyle, Essentials of robust control, Vol. 104, Prentice Hall, Upper Saddle River, NJ, 1998.

[36] C.-Y. Kao, B. Lincoln, Simple stability criteria for systems with time-varying delays, Automatica 40 (8) (2004) 1429–1434.

[37] Y. Nesterov, A. Nemirovskii, Interior-point polynomial methods in convex programming, Philadelphia, P.A: SIAM, 1994.

[38] P. Gahinet, A. Nemirovski, A. Laub, M. Chilali, LMI control toolbox, The MathWorks Inc. 1995.

[39] Y. Labit, D. Peaucelle, D. Henrion, Sedumi interface 1.02: a tool for solving LMI problems with sedumi, in: IEEE International Symposium on Computer Aided Control System Design, 2002, pp. 272–277.